PDA Journal
of Pharmaceutical Science and Technology

Single-Use System Integrity IV: A Holistic Approach Based on Compiled Scientific Study Data

Marc Hogreve

PDA J Pharm Sci and Tech **2023**, *77* 133-144
Access the most recent version at doi:10.5731/pdajpst.2022.012794

RESEARCH

Single-Use System Integrity IV: A Holistic Approach Based on Compiled Scientific Study Data

MARC HOGREVE

Product Development, Sartorius Stedim Biotech GmbH, Goettingen, Germany

ABSTRACT: This concluding article of the publication series provides an overarching summary of all study results presented in the three previous articles (1–3). Their interdependency in achieving a holistic approach to the integrity assurance of single-use systems (SUSs) employed in (bio)pharmaceutical manufacturing is finally illustrated. Two of those three studies were conducted to understand microbial ingress and liquid leak mechanisms in polymeric film material as determinants of the maximum allowable leakage limit (MALL) for SUSs using artificially created defects. The third study characterized gas flow through these defects—an essential variable for robust validation of physical integrity test methodologies based on gas flow. In all studies, the test samples used were 50 mm round patches of two ethylene vinyl acetate (EVA) multilayer films (300 µm and 360 µm thick) and a polyethylene (PE) multilayer film (400 µm thick). More than 1400 test samples with artificially created leaks were used in sizes ranging from 1 µm to 130 µm. The leaks were laser-drilled into the center of each patch. Microbial ingress and liquid leak testing under various process conditions resulted in a MALL of 2 µm for microbial integrity and the prevention of liquid leakages under most severe use-case conditions. The studies also demonstrated a close relationship between the occurrence of liquid leakage and microbial contamination. Different model solutions were used to evaluate the impact of liquid characteristics, mainly surface tension. The data were applied to build mathematical models for predicting the MALL under any intended use-case condition. By characterizing gas flow behavior over a broad pressure range using various defect sizes, it was possible to create formulas for three different flow regimes. These were suitable for calculating leak size in a defective product directly from the corresponding flow rate or vice versa. Finally, compilation of these different aspects enabled the authors to design and validate non-destructive physical integrity test methods having detection limits correlated to the MALL for SUSs.

KEYWORDS: Single-use system (SUS), single-use system integrity (SUSI), maximum allowable leakage limit (MALL), microbial ingress testing, liquid leak testing, gas flow rate through microchannels.

Introduction

Given the expansion of single-use systems (SUSs) in all process steps of commercial manufacturing, integrity failure can significantly impact drug safety, availability, and costs. Leaks are among the top three concerns in the (bio) pharmaceutical industry (4) that prevent further expansion of SUSs. If present, leaks can create harmful product loss, production and planning disruptions, and product shortages. If the product is hazardous (e.g., viruses), operator and environmental safety risks are posed. Looking at SUSs used in (bio)pharmaceutical processes, a consistent robustness and risk-based integrity testing strategy can enhance process, product, and/or patient safety. Consequently, SUS integrity (SUSI) has become a critical quality attribute for both end users and suppliers. Over the past years, increasing industry scrutiny has been focused on SUSI, raising the need to develop robust scientific models on which to base liquid leakage and microbial ingress mechanisms to implement appropriate physical integrity and leak testing technologies.

There is a relevant difference between physical leak testing and integrity testing. Whereas leak testing only identifies leaks of any size and is used to mitigate the risk of

Corresponding Author: Product Development, Sartorius Stedim Biotech GmbH, August-Spindler-Strasse 11, 37079 Goettingen, Germany; Telephone +49.551.308.3752; Fax +49.551.308.2062; Email: marc.hogreve@sartorius.com
doi: 10.5731/pdajpst.2022.012794

an integrity failure, physical testing that has a detection limit correlated to the barrier properties of the SUS can provide a full integrity guarantee and is called an integrity test. If the barrier property of the SUS is designed to prevent any entry of detrimental contaminants, that is, microorganisms, the physical integrity test should be able to find defects with sizes that may lead to microbial contamination during use of the SUS. For SUSs with the barrier property to avoid liquid leakages, for example, if the content is toxic and could compromise the operator or environmental safety, the same applies accordingly. For that reason, it is important to understand microbial ingress and liquid leak mechanisms through defects in SUSs under use-case conditions. For reliable validation of physical test methods, it is also important to understand the relationship between the leak geometry and the gas leak rate.

As indicated in the previous articles, valuable studies related to physical and microbiological integrity testing were performed in the past decades, but have mostly evaluated the integrity of rigid packages like glass vials (5–8) or food cans (9, 10). Studies on flexible bags like retort pouches (11–13) are similarly available, but none were conducted using actual SUS material and use-case conditions. The same is true for studies related to defects causing liquid leakages in flexible packaging. Either studies are related to microbial testing, like the one conducted by Moghimi et al. (13, 14) on flexible pouches, or they were done on rigid material, like the one by Mala and Li (15), which studied the flow characteristics of water in microtubes of fused silica and stainless steel and with diameters of 50 µm to 254 µm. For all these reasons, it was needed to initiate scientific studies to characterize microbial ingress and liquid leakage mechanisms for material typically used in SUS bag assemblies.

Finally, the relation between a geometrical defect size and the corresponding flow rate is theoretically known and has also been reported in a table in <USP 1207> (16), showing the relation between a perfect hole of negligible length and the air flow rate passing through this hole at a pressure difference of 1 atm and a temperature of 25°C. But, as mentioned there, the relation is based on theoretical approximations and is not definitive. To the authors' knowledge, this approximation is based on experiments done with laser-drilled defects in aluminum foil of 125 µm thickness. This must not necessarily represent the behavior of polymeric material used for the assembly of SUSs.

For all the previously mentioned reasons, it was essential to launch scientific studies to better understand the specific characteristics of microbial ingress and liquid leakage mechanisms as well as the flow dynamics in said polymeric materials.

Materials and Methods

Two different studies, one on liquid leakage and the other on microbial ingress, were conducted to identify the maximum allowable leakage limits (MALLs) at which microbial contamination into and liquid loss out of SUSs is prevented. The determination of the SUS-specific MALLs under use-case conditions relevant to SUSs, that is, using a microbial challenge test by aerosolization instead of immersion, is important, because it better reflects the environmental conditions in which SUSs are typically used. Therefore, one prerequisite is to define the respective test method parameters accordingly. The definition of the pressure range is common to both microbial ingress testing and liquid leakage testing. As shown in Figure 1, the pressure range of 0–300 mbar used for this testing was representative and covered the most severe use-case conditions of SUSs. Typical use-cases for SUSs are liquid storage, mixing, and shipping. Although the hydrostatic pressure of the liquid column is relevant for storage applications, dynamic pressure pulses need to be considered for mixing and shipping applications. These pressure levels were identified for mixing applications by computer fluid dynamics (CFD) simulation and for shipping conditions by recording of shocks and accelerations sustained during real-life liquid shipping validation trials. The selection of further test method parameters unique to each study is described in the next paragraph.

In addition, a third study was conducted to establish a correlation between geometrical leak size and leak rate. The official definition of MALL for SUSs given in several ASTM standards (17–19) highlights the relevance of this correlation. This correlation is specifically important when the validation of physical integrity test methods is concerned, for example, pressure decay or helium tracer gas testing. The scientific work published in the previous articles of the series encompassed three main SUS integrity studies:

1. A microbial ingress study to identify MALLs under real process conditions. For that purpose, a robust microbial aerosol method was developed, challenging a high quantity of test samples with a high microbial challenge concentration at different pressures. The aim was to understand the microbial ingress mechanism in SUS materials and correlate MALLs for microbial ingress to detection limits of physical integrity test methods (1).

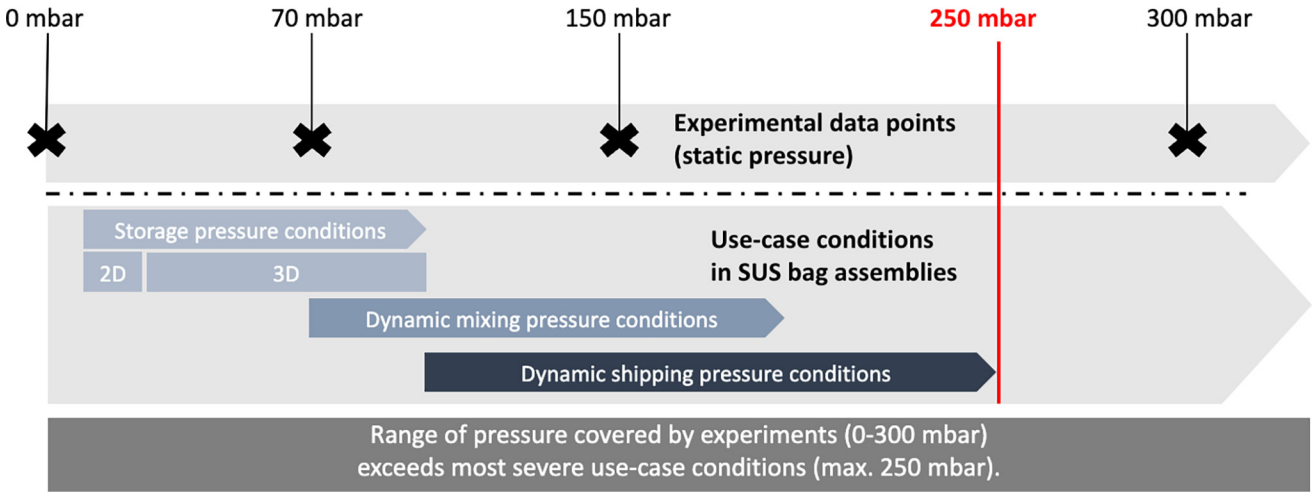

Figure 1

Pressure ranges used for integrity science studies.

2. A liquid leak study to determine the MALLs for liquid leakage using different defect sizes in film patches with different model solutions at different pressures (2).

3. A gas flow rate study to determine the relation between gas flow rate and differential pressure for various defect sizes that produce different flow regimes (3).

Test Setups

For all three studies, test samples were created from film patches of 50 mm in diameter made from ethylene vinyl acetate (EVA) multilayer films (300 µm and 360 µm thick) and a polyethylene (PE) multilayer film (400 µm thick). Defects were artificially created by laser drilling and calibrated by flow rate.

For the microbial ingress tests by aerosolization (Study I), a test method with an aerosolization chamber (Figure 2A) was developed to create a test setup that homogeneously, reproducibly, and reliably delivers a high concentration of microorganisms still viable at the end of the aerosol cycle to a high amount of test samples per run. A high challenge concentration of 10^6 CFU/cm^2, derived from ISO7 clean room specifications and augmented by

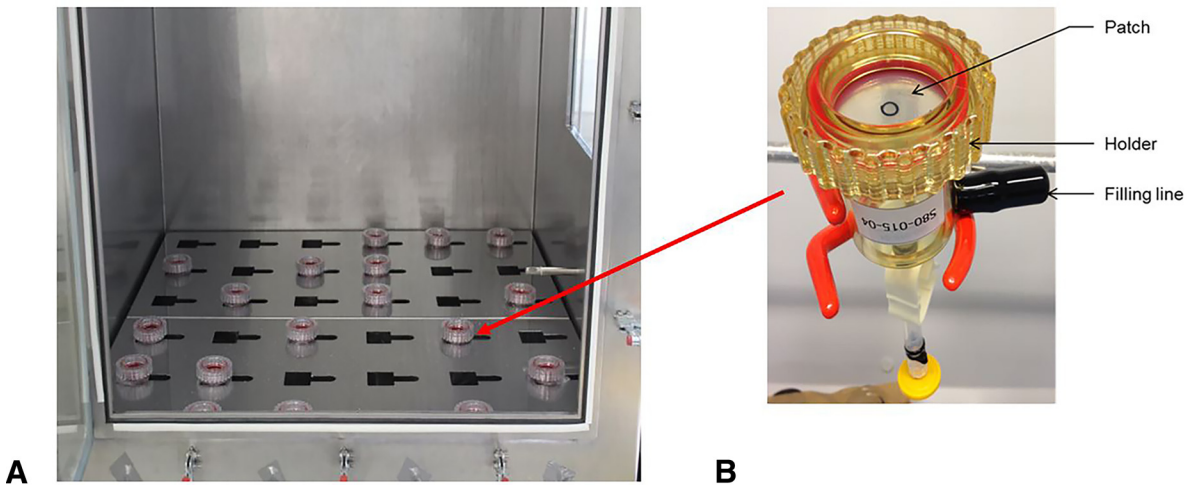

Figure 2

Test setup (A) and test sample (B) for microbial ingress testing.

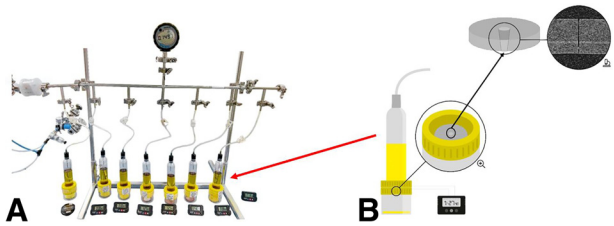

Figure 3

Test setup (A) and test sample (B) for liquid leakage testing.

6 logs, was used to challenge the test samples. Up to 36 test samples (Figure 2B) with artificial defects of various sizes were tested in parallel, including positive and negative controls. Test samples were pressurized to defined pressure differentials of 70 mbar, 150 mbar, and 300 mbar or tested without any pressure. After an aerosol exposure duration of 3 h, the test samples were incubated for 14 days at 30˚C–35˚C and visually inspected for growth.

Test samples (Figure 3B) used for the liquid leak tests (Study II) had artificial defects of various sizes and were filled with liquid, pressurized, and kept for up to 30 days under static pressure. Pressure levels were identical to those of the microbial ingress study. Indicator paper and a stopwatch-controlled electronic circuit were used to identify the presence of leakage and the leakage time of the first droplet. Only if no single droplet was observed during the period of 30 days was a test sample considered to have no leakage. Different model solutions were used to evaluate the impact of surface tension on the results.

To correlate flow rates to geometrical defect size (Study III), polymeric film patches with artificial defects of various sizes were mounted in a patch holder with their nominal defect size on the downstream side. On the upstream side, a pressure controller and a stainless-steel volume were used to apply a constant pressure, while on the downstream side a laminar flow element was used to measure the flow rate. To permit particles to block the pinhole, a 0.2 µm filter was installed between the volume and the holder (Figure 4). Several differential pressures in the range of 0 mbar to 1000 mbar were used to establish different flow regimes.

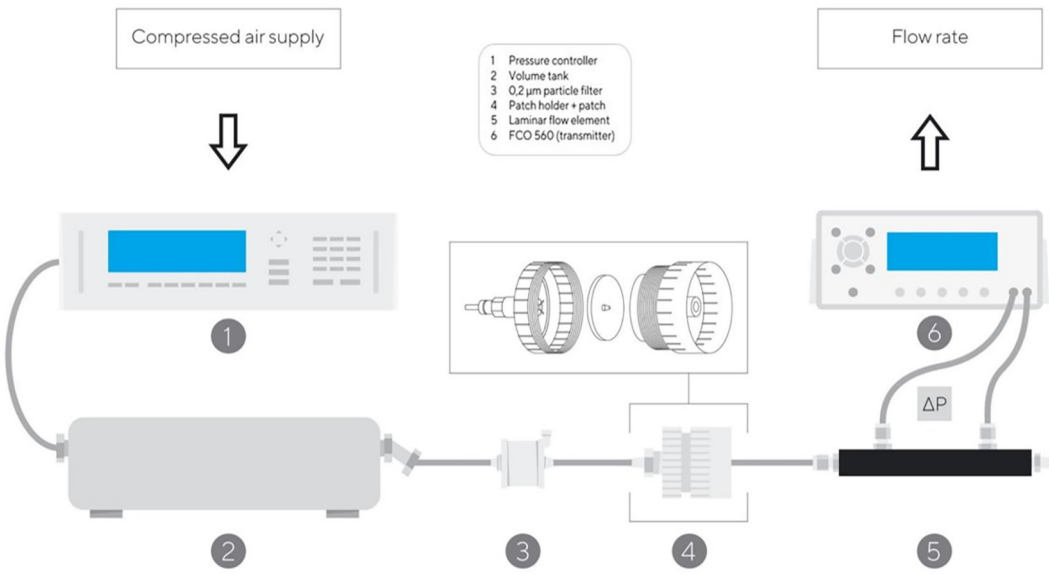

Figure 4

Test setup for flow rate measurement.

A more detailed description of test setups, test methods, and the test sample designs of the three studies can be found in the respective prior PDA journal articles (1–3).

Test Principles and Data Analysis

As the mechanisms examined in the two studies (I and II) to identify the MALLs were based on different principles, that is, microbial ingress is a probabilistic phenomenon and liquid leakage is a physical phenomenon, the sampling of test samples and data analyses were different, too. For the microbial ingress study, a high number of 30 test samples per combination of film type, defect size, and pressure were tested for the two extreme pressure conditions to obtain meaningful statistical data. Based on initial data, further testing was conducted with fewer test samples using a three-phase optimal design (3POD) algorithm for experimental planning. This algorithm is very useful for planning experiments with binary results, that is, growth or no growth (20). Due to the probabilistic behavior, the MALLs were calculated based on probability, considering the whole data set for each combination. For this reason, test samples showing microbial ingress were not necessarily classified as critical based on nominal defect size.

Liquid leakage is considered a deterministic phenomenon because it depends on defect size, surface tension of the liquid, and the applied pressure. Therefore, initially only triplets of test samples for combinations with the worst-case pressure were tested. Based on these initial data, a Design of Experiments (DoE) was used for further testing and finally not all combinations were tested. From one triplet, a single test sample showing a leak was sufficient to classify the nominal defect size of the triplet as critical. The MALL was identified considering only the largest nominal defect size for which no test sample had shown leakage and no further leakage detected for smaller defect sizes. In both studies, the experimentally determined and statistically calculated MALLs were used to generate the mathematical model to predict the MALL for pressure conditions between the experimental data points.

Results and Discussion

To give a conclusion of the overall result, the exemplary data of each individual study, relevant for evaluating the interdependencies between the different studies, is first presented and discussed. Compared with the data on atmospheric pressure and a pressure differential of 300 mbar as shown in the first publication of this series, additional data on microbial ingress testing at differential pressures of 70 mbar and 150 mbar were added to this evaluation.

TABLE I
Number of Test Samples per Pressure and Film Type

Pressure (Mbar)	0	70	150	300
EVA (300 µm)	288	45	45	150
PE (400 µm)	288	194	45	150
Total	**1205**			

EVA, ethylene vinyl acetate; PE, polyethylene.

Next, the relationship between microbial ingress and the presence of liquid leakages is described and use-case specific MALLs identified. Finally, to derive threshold leak rate limits for physical nondestructive testing, the results from the destructive microbial ingress tests and liquid leakage tests are correlated to flow rate by applying the flow regimes established in the third study.

Experimental Results of the Microbial Ingress Testing Study

In total, 1205 test samples were used to determine the MALLs for microbial contamination under various use-case conditions (Table I). For the EVA films, only a thickness of 300 µm was tested because the shorter path length of the defect was considered worst-case. Differences in sampling per combination of pressure and film type are attributable to the approach explained in the previous paragraph.

All data were analyzed with the following steps:

1. Find the experimental defect size for which the first microbial growth was detected

2. Calculate the sample proportion (%), that is, the number of samples showing microbial growth at the defined defect size divided by the number of total tests conducted on this defect size

3. Analyze the whole dataset with transformed logistic regression

4. Find the probability of having growth for the same defect size

TABLE II
Bacterial Growth vs total Number of Test Samples per Film Type and Test Pressure

Pressure	0		70		150		300	
Film Type	EVA	PE	EVA	PE	EVA	PE	EVA	PE
Nominal defect size [µm]	Bacterial Ingress/Total Samples							
1			0/7	0/2	0/1	0/5	0/30	0/30
2	0/18	0/18	0/8	0/2	0/2	0/6	0/30	2/30
3			1/6*	0/1	0/2	2/4	8/30	2/30
4			0/1	0/3	1/5			
5			0/1	0/34	0/4	2/4	17/30	10/30
6				0/2	1/3			
7				0/1	1/1	1/1		
8			2/3	2/6		1/3		
9				0/2				
10	0/30	0/30	0/1	1/31	1/5	0/2		
12					1/1			
13				1/1				
15	0/30	0/30	1/1	30/31	1/2	3/4		
16				1/1				
17					1/1			
20	0/30	1/30*	0/1	31/31	2/3	1/1		
25	0/30	0/30	1/1	31/31		1/1		
30	0/30	0/30	1/1	1/1	2/2	3/3		
35					1/1			
40	1/30	0/30	1/1	1/1	2/2	3/3		
50	1/30	6/30	1/1	4/4	3/3	4/4		
60			3/3	3/3	2/2	1/1		
70			3/3		1/1	1/1		
75				1/1				
80	14/30	15/30		2/2	1/1			
90			3/3	1/1	1/1			
100	14/30	22/30	1/1	1/1		1/1		
110			1/1	1/1				
120					1/1	1/1		
130					1/1			
150			1/1					

EVA, ethylene vinyl acetate; PE, polyethylene.

5. Compare the two probabilities

Table II provides an overview of all test results, indicating the amount of test samples showing microbial growth compared with the total number of samples tested. The use of a 3POD algorithm as an iterative statistical planning tool produced individual defect size distributions for the different testing combinations. The values in bold show the smallest defect sizes exhibiting microbial ingress. For higher test pressure of 150 mbar and 300 mbar, this is in the range of 2 µm to 5 µm. As the test pressure drops, the smallest defect size permitting microbial growth increases. Some results were questioned as outliers, especially when a single microbial growth was observed for defect sizes where the next larger ones did not show growth, indicated by "*" in Table II. Ultimately, however, this question turned out to be moot because, by nature, logistic regression considers all samples to calculate the probability of growth, and a

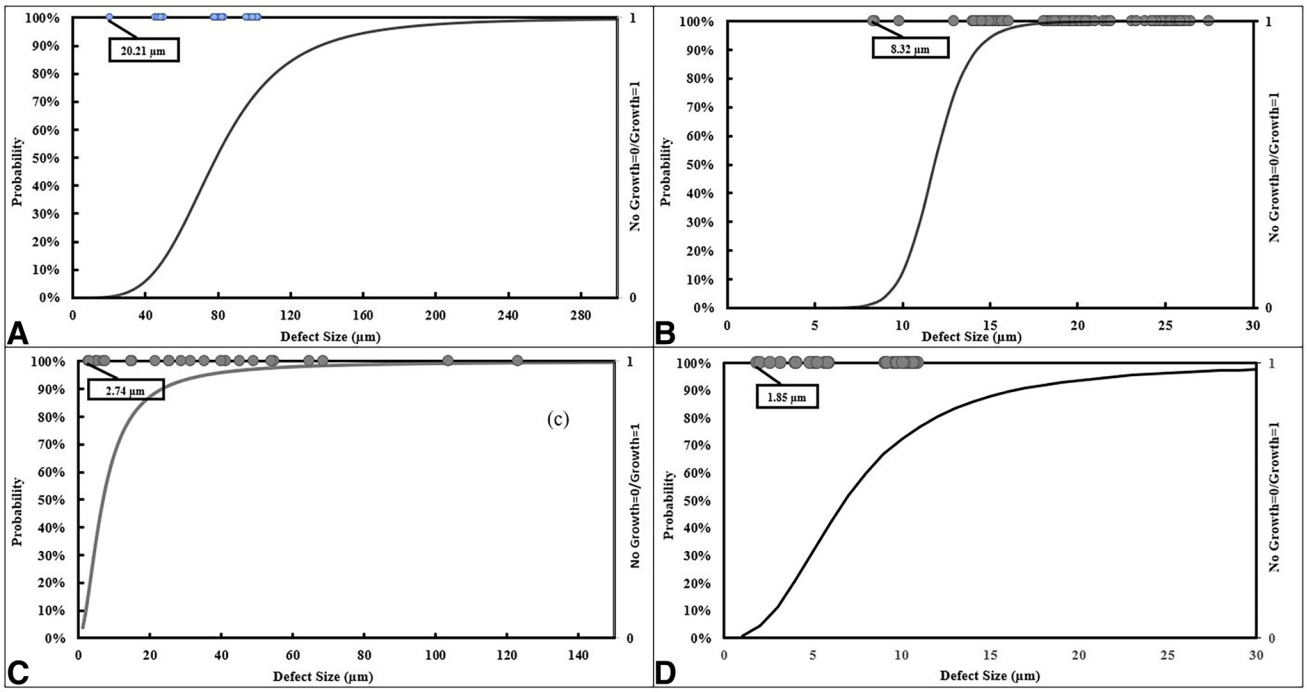

Figure 5

Probability curves for microbial ingress in polyethylene film; (A) 0 mbar, (B) 70 mbar, (C) 150 mbar, and (D) 300 mbar.

single growth cannot significantly change the probability curve.

As an example, Figure 5 shows the four graphs representing the probabilities for defects in PE film to permit microbial contamination. The value in the box indicates the smallest defect size that led to microbial ingress for experimental testing at the respective test pressure. This defect size could usually be seen as critical, and the MALL should be defined below. However, as already mentioned, the MALL for microbial ingress is defined according to the probability of microbial contamination given the probabilistic nature of the microorganisms.

TABLE III
Defect Sizes Showing a 10% Probability for Microbial Ingress

EVA Film	
Pressure (mbar)	**Defect Size (µm)**
0	56.62
70	3.62
150	4.18
300	2.00
PE Film	
0	45.87
70	9.78
150	1.96
300	2.83

EVA, ethylene vinyl acetate; PE, polyethylene

As defined in USP <1207> (16), the MALL for preserving the sterility of a drug in primary packing is the defect size for which the probability is <10%. Based on these graphs and the underlying function, Table III provides a summary of the defect sizes that permit microbial ingress with a probability of 10% for both types of film used in the experiments.

Experimental Results of the Liquid Leak Testing Study

As shown in Table IV, 135 test samples were used to determine the MALLs for liquid leakages under various use-case conditions in this study. Again, differences in sampling per combination of pressure, model solution, and film type derive from the approach explained for sampling and data analysis. Also, some additional data to those published in the second article of this publication series are presented.

TABLE IV
Number of Test Samples per Pressure, Model Solution, and Film Type

Pressure (Mbar)	70		150		300	
Model Solution	Water	TSB	Water	TSB	Water	TSB
EVA (300 µm)	6	6	-	6	6	6
EVA (360 µm)	6	6	3	12	6	6
PE (400 µm)	18	15	-	3	15	15
Total	135					

EVA, ethylene vinyl acetate; PE, polyethylene; TSB, tryptic soy broth.

Table V summarizes all test results, indicating the amount of test samples with liquid leakage compared with the total number of samples tested. In addition to the binary result of leakage or no leakage, the time it took for the first droplet to form outside the defect channel was recorded. For simplicity's sake, the data reported in the second article of this series (2) are not presented here. The use of DoE resulted in not testing all possible combinations of film type, model solution, defect size, and pressure. The values in bold represent the smallest defect sizes showing liquid leakage. For all combinations tested at 150 mbar and 300 mbar using a defect size of 3 µm, this was the smallest one that produced liquid leakage. At 70 mbar test pressure, the smallest defect size showing liquid leakage across all combinations was 5 µm. For all tested combinations, 2 µm was the defect size not showing any liquid leakage. Given that the phenomenon of liquid leakage should be purely based on physical parameters, the results showing leakage in only a fraction of the tested samples raised some questions. To explain any deviation from the expected results, microscopic investigations, including

TABLE V
Liquid Leakages vs Total Number of Test Samples per Film Type, Model Solution, and Test Pressure

Model Solution		Water			TSB		
		No. of Leaking Samples /No. of Tested Samples			No. of Leaking Samples /No. of Tested Samples		
Applied Pressure (Mbar)	Nominal Defect Size (µm)	EVA 300 µm	EVA 360 µm	PE 400 µm	EVA 300 µm	EVA 360 µm	PE 400 µm
300	10	**3/3**	3/3	5/6	**3/3**		
	5			3/3		0/3	4/6
	3		**3/3**	**3/3**			**6/6**
	2	0/3		0/3	0/3	0/3	0/3
150	10						
	5		0/3			**6/12**	
	3				**1/3**		
	2				0/3		0/3
70	25			3/3			3/3
	20			3/3			
	15			3/3			3/3
	10	**3/3**	**3/3**	3/3	**2/3**	**1/3**	3/3
	5			**3/3**			**3/3**
	3						0/3
	2	0/3	0/3	0/3	0/3	0/3	

EVA, ethylene vinyl acetate; PE, polyethylene; TSB, tryptic soy broth.

light microscopy and computed tomography, were used to interpret and understand the physics and geometries of the microchannels. Again, more details can be found in the respective articles. Contrary to the definition of the MALL for microbial ingress, the largest defect size not showing any liquid leakage was considered as the MALL for the individual combination of testing conditions for this study.

Experimental Results of the Flow Rate Testing Study

A total of 171 PE and EVA film patches were tested with several pressure differentials between 50 mbar and 1000 mbar. Artificial defects with sizes between 2 µm and 100 µm were introduced into the film patches by laser drilling. According to the DoE, an increased number of samples were used at the center point 30 µm and the corner points 2 µm and 100 µm. In addition to a single measurement for each patch and differential pressure, repetitive measurements were taken on one patch per defect size under all differential pressures to check test setup reliability and increase data validity. This led to a total of 1496 measurements. The general behavioral dependency of the measured gas flow rate through different defect sizes at various differential pressures was logical.

Based on knowledge of existing gas flow regimes, that is, Knudsen flow, viscous flow for tubes, and viscous flow for orifices, different parameters were evaluated to correlate defect size to gas flow rate under the given testing conditions. These parameters were pressure differential, leak size, and leak geometry. As described in more detail in the third article of this publication series, these parameters have different impacts on the flow rate depending on the flow regime. All results were used to build three different formulas (eqs 1–3) based on known flow regimes but with material and defect-specific correction factors to achieve the best fit of correlation between defect size and gas flow rate.

Knudsen Flow:

$$Q = \left(\frac{p_1}{p_2} - 1\right)\bar{c}{R_{out}}^2\sqrt{\frac{\pi}{2}}\left(\frac{R_{in}}{R_{out}}\right)^{\kappa-1} \quad (1)$$

Viscous Flow, Tube

$$\left(\frac{l}{R_{in}+R_{out}} > 5\right):$$

$$Q = \left(\frac{p_1}{p_2} - 1\right)^z\bar{c}{R_{out}}^2\sqrt{\frac{\pi}{16}}\left(\frac{R_{in}}{R_{out}}\right)^{\kappa} \quad (2)$$

Viscous Flow, Orifice

$$\left(\frac{l}{R_{in}+R_{out}} < 4\right): Q = \left(\frac{p_1}{p_2} - 1\right)^z\bar{c}{R_{out}}^2\sqrt{2\pi}\left(\frac{R_{in}}{R_{out}}\right)^{\frac{\kappa-1}{2}} \quad (3)$$

Mathematical Models for Predicting MALLs of SUSs

Finally, to build mathematical models for predicting the MALL of SUSs under any use-case condition, the first step was to analyze the correlation between microbial ingress and liquid leakage. Results discussed in the second article of this publication series had already indicated a good fit between data showing the ability to

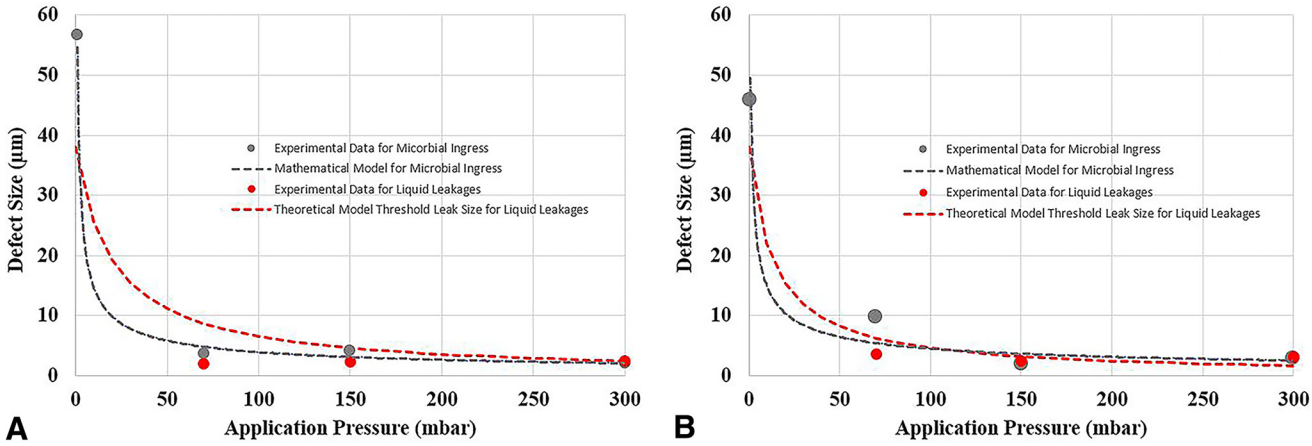

Figure 6

Experimental data and models comparing microbial ingress and liquid leakage; (A) ethylene vinyl acetate film and (B) polyethylene film.

permit microbial ingress and liquid leakages. Figure 6 summarizes all experiments with the following:

1. Experimental data for which microbial ingress was observed with a probability of 10%

2. The mathematical model, by power fit, that predicts the defect size for which microbial ingress can be expected with a probability of 10% at any use-case pressure in the given range

3. Experimental data on the largest defect size for which no liquid leakage was observed

4. The theoretical model of threshold leak size (transition from leaking to non-leaking) based on eq 4 with a material specific factor α for each film, determined to obtain the best fit to the experimental data

$$P_0 > P_{atm} + \left({}^{2\sigma}/_{r} - \rho g L\right).\alpha \qquad (4)$$

σ: surface tension of the liquid

r: radius of the droplet

ρgL: the hydrostatic pressure of the column of liquid, where ρ is the density of the liquid, g the acceleration of gravity, and L the height of the liquid

P_0: applied pressure, given as an absolute pressure

Pa: atmospheric pressure

α: empirical factor

Based on these data, the defined barrier properties, and the use-case pressure ranges shown in Figure 1, the MALL can be determined for a specific SUS used in a defined application, for example, a 500 L 3 D bag assembly for liquid shipping of sterile drug substance. This forms the basis for implementing meaningful integrity test methods.

Validation of Physical Test Methods Based on Flow

Knowing the MALLs for SUSs provides the target detection limits for integrity testing and enables claiming that a tested SUS maintains the defined barrier properties. In terms of defining the MALLs for microbial ingress and liquid leakage, the gas flow rate through a specific defect size is not of interest; rather, it is important for the validation of physical test methods to achieve a direct correlation to the barrier property of interest. This is true for all pressure- and flow-based test methods using gases, for example, pressure decay or helium tracer gas.

To reliably prove the ability of a test method to detect the defect size of concern, negative controls (integral test samples) and positive controls (test samples with artificially created defects) must be used. These positive controls can be quantified either by microscopic imaging, or more reliably, by flow-calibration. It is a fact that a flow is not only linked to the differential pressure, but that the characteristic can also change between typical calibration conditions, for example, measuring the flow rate at 1000 $mbar_g$ against 1 atm, and the actual testing conditions, for example, 300 $mbar_g$ against 1 $mbar_a$ for tracer gas testing in vacuum mode. Therefore, established formulas can help verify the measured flow rate results. Finally, an appropriate acceptance criterion to reliably differentiate conforming from nonconforming SUSs can be selected by applying statistical calculation to average values and standard deviation to the distributions of positive and negative controls.

Conclusion

Understanding microbial ingress and liquid leakage mechanisms of polymeric material used for manufacturing SUSs is the basis for the implementation of valuable and meaningful physical integrity test methods. Based on experimental data indicating the defect sizes that permit microbial contamination or produce liquid leakage under defined use-case conditions, mathematical models can be defined to predict the MALL for a SUS used under any application-specific conditions.

All experiments conducted and compiled here have shown that the parameter having the greatest influence on the defect size considered as the MALL is pressure. Other parameters like material type, channel length, or liquid surface tension have minor impact. Also, the results from microbial ingress and liquid leakage tests show a close correlation. This confirms the assumption that liquid must be present in the defect channel to allow microbial ingress even against the direction of pressure differential.

For the most severe use-case conditions of liquid shipping in large-volume 3D bag assemblies, the MALL to confirm the barrier properties of avoiding microbial contamination and liquid leakages is 2 µm for both types of film tested here. Finally, implementing 100% integrity testing using a nondestructive physical test method with a detection limit correlated to the identified MALL based on sound scientific data provides the highest level of integrity assurance for a SUS used under its intended use-case conditions.

Conflict of Interest Declaration

The author declares that they have no competing interests.

References

1. Aliaskarisohi, S.; Hogreve, M.; Langlois, C.; Cutting, J.; Barbaroux, M.; Cappia, J.-M.; Menier, M.-C. Single-Use System Integrity I: Using a Microbial Ingress Test Method to Determine the Maximum Allowable Leakage Limit (MALL). *PDA J. Pharm. Sci. Technol.* **2019**, *73* (5), 459–469.

2. Aliaskarisohi, S.; Kumar, C.; Hogreve, M.; Montenay, N.; Cutting, J.; Mundrigi, A.; Paramathma, A. Single-Use System Integrity II: Characterization of Liquid Leakage Mechanisms. *PDA J. Pharm. Sci. Technol.* **2021**, *75* (3), 258–272.

3. Aliaskarisohi, S.; Urbaniak, T.; Hogreve, M. Single-Use System Integrity III: Gas Flow Rate through Laser-Drilled Microchannels in Polymeric Film Material. *PDA J. Pharm. Sci. Technol.* **2022**, *76* (1), 9–18.

4. BioPlan Associates, 18th Annual Report and Survey of Biopharmaceutical Manufacturing Capacity and Production, 2021.

5. Chen, C.; Harte, B.; Lai, C.; Pestka, J.; Henyon, D. Assessment of Package Integrity Using a Spray Cabinet Technique. *J. Food Prot.* **1991**, *54* (8), 643–647.

6. Kirsch, L. E.; Nguyen, L.; Moeckly, C. S. Pharmaceutical Container/Closure Integrity I: Mass Spectrometry-Based Helium Leak Rate Detection for Rubber-Stoppered Glass Vials. *PDA J. Pharm. Sci. Technol.* **1997**, *51* (5), 187–194.

7. Nguyen, L. T.; Muangsiri, W.; Schiere, R.; Guazzo, D. K. M.; Kirsch, L. E. Pharmaceutical Container/Closure Integrity IV: Development of an Indirect Correlation between Vacuum Decay Leak Measurement and Microbial Ingress. *PDA J. Pharm. Sci. Technol.* **1999**, *53* (4), 211–216.

8. Burell, L. S.; Carver, M. W.; DeMuth, G. E.; Lambert, W. J. Development of a Dye Ingress Method to Assess Container-Closure Integrity: Correlation to Microbial Ingress. *PDA J. Pharm. Sci. Technol.* **2000**, *54* (6), 449–455.

9. Gilchrist, J. E.; Rhea, U. S.; Dickerson, R. W.; Campbell, J. E. Helium Leak Test for Micron-Sized Holes in Canned Foods. *J. Food Prot.* **1985**, *48* (10), 856–860.

10. Bankes, P.; Stringer, M. F. The Design and Application of a Model System to Investigate Physical Factors Affecting Container Leakage. *Int. J. Food Microbiol.* **1988**, *6* (4), 281–286.

11. Gilchrist, J. E.; Shah, D. B.; Radle, D. C.; Dickerson, R. W. Jr. Detection in Flexible Retort Pouches. *J. Food Prot.* **1989**, *52* (6), 412–415.

12. Keller, S. W.; Marcy, J. E.; Blakistone, B. A.; Lacy, G. H.; Hackney, C. R.; Carter, W. H. Jr. Bioaerosol Exposure Method for Package Integrity Testing. *J. Food Prot.* **1996**, *59* (7), 768–771.

13. Moghimi, N.; Kim, S.-J.; Park, S.-I. Assessing of Flexible Packaging Integrity: Using the Aerosolization Bacteria. *Packag. Technol. Sci.* **2016**, *29* (3), 135–143.

14. Moghimi, N.; Park, S.-I. Leakage Assessment of Flexible Pouches Using Dye Penetration Test with Correlation to Modeled Bacterial Aerosol Challenge Test. *Food Sci. Biotechnol.* **2017**, *26* (4), 947–953.

15. Mala, G. M.; Li, D. Flow Characteristics of Water in Microtubes. *Int. J. Heat Fluid Flow* **1999**, *20* (2), 142–148.

16. U.S. Pharmacopeial Convention, General Chapter <1207> Sterile Product Packaging - Integrity Evaluation. In *USP 39–NF 34*, USP: Rockville, MD, 2016.

17. ASTM International, *E3244-20 Standard Practice for Integrity Assurance and Testing of Single-Use Systems*. ASTM: West Conshohocken, PA, 2020.

18. ASTM International, *E3251-20 Standard Test Method for Microbial Ingress Testing on Single-Use Systems*. ASTM: West Conshohocken, PA, 2020.

19. ASTM International, *E3336-22 Standard Test Method for Physical Integrity Testing of Single-Use Systems*. ASTM: West Conshohocken, PA, 2022

20. Wu, C. F. J.; Tian, Y. Three-Phase Optimal Design of Sensitivity Experiments. *J. Stat. Plan. Inference* **2014**, *149* 1–15.

PDA Journal
of Pharmaceutical Science and Technology